Available online at www.sciencedirect.com
ScienceDirect
C. R. Physique 10 (2009) 660–675
COMPTES RENDUS PHYSIQUE

Physics and heritage / Physique et patrimoine

Accelerators and x-rays in cultural heritage investigations

Heinz-Eberhard Mahnke [a,b,c,*], Andrea Denker [b], Joseph Salomon [a,1]

[a] *Centre de recherche et de restauration des musées de France, CNRS UMR-171, palais du Louvre, 14, quai François-Mitterrand, 75001 Paris, France*

[b] *Helmholtz-Zentrum Berlin für Materialien und Energie, Glienicker Str. 100, 14109 Berlin, Germany*

[c] *Freie Universität Berlin, Fachbereich Physik, Arnimallee 14, 14195 Berlin, Germany*

Available online 12 October 2009

Abstract

In the following article a review is given on the use of accelerators in studies connected to our cultural heritage. It focuses on making use of the production and detection of x-rays as a general tool. At "small accelerators", the proton induced x-ray emission (PIXE), especially when combined with Rutherford backscattering spectroscopy (RBS), has been developed to a very versatile and powerful technique for near-surface investigations. It is well complemented by larger facilities, synchrotron radiation sources as well as medium energy ion accelerators for high energy PIXE. With the development of small compact electron accelerators, a new generation of mono-energetic high-energy high-intensity x-ray sources will add a very comfortable complement in cultural heritage studies. ***To cite this article: H.-E. Mahnke et al., C. R. Physique 10 (2009).***
© 2009 Académie des sciences. Published by Elsevier Masson SAS. All rights reserved.

Résumé

Accélérateurs et rayons X en recherche sur le patrimoine culturel. Cet article présente un aperçu des accélérateurs utilisés dans des études reliées à notre patrimoine culturel, avec un intérêt particulier pour la production et la détection des rayons X comme technique générale. Le développement des « petits accélérateurs » pour l'utilisation des rayons X produits par des protons (PIXE) combinée avec la spectrométrie en rétrodiffusion de *Rutherford* (*RBS*) a conduit à une technique adaptable et puissante pour l'analyse des couches superficielles. Des techniques complémentaires existent dans des installations plus grandes comme des sources de radiation synchrotron ou encore des accélérateurs d'énergie moyenne pour le PIXE de haute énergie. Le développement d'accélérateurs petits et compacts comme source intense de rayons X de haute énergie ajoutera un complément confortable pour les études de notre patrimoine. ***Pour citer cet article : H.-E. Mahnke et al., C. R. Physique 10 (2009).***
© 2009 Académie des sciences. Published by Elsevier Masson SAS. All rights reserved.

Keywords: X-ray fluorescence (XRF); PIXE; Non-destructive analytics; Cultural heritage; Inverse Compton source

Mots-clés : Fluorescence de rayons X (XRF) ; PIXE ; Analyse non-destructive ; Patrimoine culturel ; Source par effet Compton inverse

* Corresponding author at: Helmholtz-Zentrum Berlin für Materialien und Energie, Glienicker Str. 100, D-14109 Berlin, Germany.
E-mail address: mahnke@helmholtz-berlin.de (H.-E. Mahnke).

[1] In the course of preparing this review our colleague Joseph Salomon passed away on February 3, 2009. We not only miss his skills on accelerators and ion beam techniques, but beyond that we miss him as a friend and colleague.

1631-0705/$ – see front matter © 2009 Académie des sciences. Published by Elsevier Masson SAS. All rights reserved.
doi:10.1016/j.crhy.2009.08.003

1. Introduction

For the understanding and conservation of objects of our cultural heritage, the context from where they originate, their historical background, their intercultural relationship, their social context and many other aspects, it is absolutely needed to "look" underneath the surface of the object after a visual inspection to obtain an image as complete as is achievable, and to determine what the object is made of to the most possible completeness. Only with knowledge about the components and their structures, as precise as possible, can a detailed study be pursued concerning the questions of art historians, archaeologists, museum conservators or curators. Of course, it is a general "must" that such investigations are done non-destructively, or by minimal invasive means. We all know from our visits to museums looking at precious paintings that they are already very sensitive to very subtle interactions with the visible light with which we illuminate the object of interest, or with the part of the electromagnetic spectrum accompanying the visible light from our light source, such as the UV or the infrared part of the spectrum.

Therefore it is crucial to optimize the tools with which the objects will be studied in terms of effectiveness in obtaining the information needed at minimal influence on the object. The minimum requirement is that there should not remain any visible change on the surface.

A widely accepted tool in cultural-heritage investigations is the well-known x-ray tube which we may consider already as an accelerator, in particular an electron accelerator, for the production of x-rays with which we want to study a precious work of art. Starting from the discussion of x-rays as delivered in tubes, we want to illustrate in the following article the necessity for investigations using larger instruments, accelerators for particles heavier than electrons and accelerators for electrons much faster than in tubes, to obtain additional information as complements to those obtained with standard x-ray tubes.

Although widely accepted as a tool for investigations, already x-rays from tubes have to be applied with care in order to prevent visible (and invisible) changes and to avoid long-term deterioration resulting from the irradiation. However, the experience with x-rays gained over many decades of investigations may serve as a guideline to overcome reservations, conservators and curators might have for investigations at accelerators.

Since the application for which the accelerator is needed deals with an art object, this object is generally not available for mounting in vacuum, with a few exceptions. Only studies in open air are easily feasible. That limits the type of radiation provided by accelerators to radiation accessible in open air. In most cases, it rules out the use of electrons, as in most electron microscopes or related techniques, or ions from heavy elements as primary sources. Thus the typical kinds of radiation easily accessible are light nuclear particles, such as protons or alpha-particles (i.e. ^{4}He-particles), as direct "radiation", or electromagnetic radiation produced as secondary type, such as x-rays or gamma-rays, which are all being used in open air. In a general sense, neutrons may also be considered as a secondary type, but we will not discuss further their use in the following, as they deserve a special description.

The development of accelerator based techniques, especially in the production of x-rays is paralleled by the achievements obtained in the development of portable x-ray systems. Since many objects to be studied cannot be brought to an accelerator, the "accelerator" has to go to the object. Therefore, there is a need for optimizing the x-ray yield and minimizing the power needed to produce it. Currently, systems with a 3-W power consumption, operating at 40 kV, are in use in field studies [1].

Typically in this context, two major types of information are requested: the *elemental composition*, perhaps with lateral and depth distribution, its determination by using accelerators will be described in greater detail; and the *visualization* of hidden structures usually based on absorption leading to tomography. The latter is the domain of x-rays, originating from standard tubes already in use. We will therefore restrict ourselves to the description of how to produce radiation by means other than tubes, and describe some special features associated with this. In some cases additional information, e.g. on the chemical and/or crystalline form may be essential for a meaningful interpretation of the context of the object. Here photon spectroscopic methods have been developed, typically using synchrotron radiation. Some of them will be briefly mentioned in this review. A full coverage concerning applications in cultural heritage studies deserves another review. In part an overview may be found in the latest special issue covering the workshop on "synchrotron radiation in art and archaeology" [2].

In the following review we will start with introducing the fundamentals of characteristic of x-rays. The coverage of the production and use of x-rays in accelerators which follows, will go beyond the already well-reviewed "small accelerators" (as an example see [3]) to larger facilities and the new perspectives for almost monochromatic x-ray

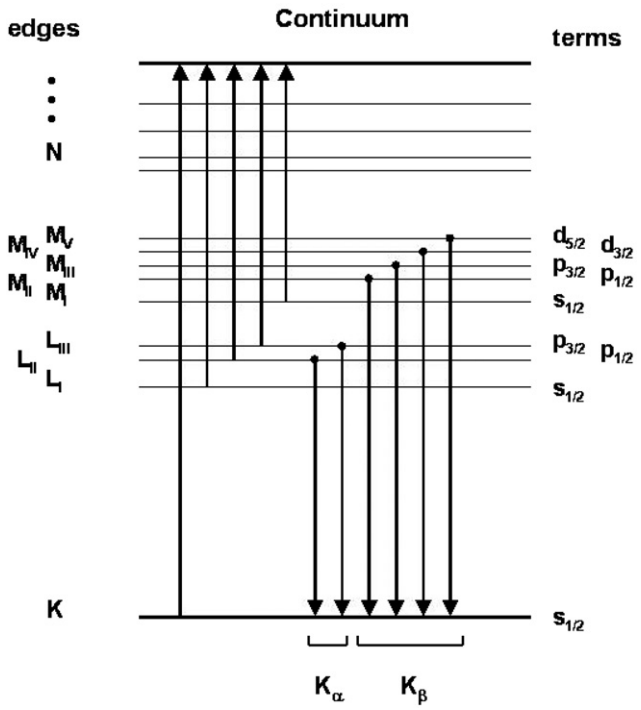

Fig. 1. Atomic level scheme with absorption and emission of x-rays, introducing the standard notations for absorption edges and x-ray lines.

sources with high intensities. It is intended to illustrate their additional potential in complementing the already existing facilities for cultural heritage related studies.

2. The x-ray signature of elements

2.1. The element number

The maxim of being most effective in elemental detection is asking for a signature to be produced with a high probability, i.e. large cross section, and with as little interference with signals from other sources as possible. Such a signature is accessible with the x-rays emitted by atoms which were excited by kicking out an inner electron either by the photo electric effect of incoming photons (x-rays or gamma radiation) or by a direct encounter with fast moving particles (electrons, ions). The excited atoms release their excess energy by emitting so-called characteristic x-rays: The energy of these x-rays increases with the element or atomic number Z as Z^2 ("Moseley's law" [4]). Thus determining the energy of emitted x-rays from the irradiated object determines the element within the object which was excited in the irradiation.

2.1.1. Characteristic x-rays and the elements

For a better understanding, some basic features on x-rays arising from electronic transitions within the atom are given here, for details the reader is referred to textbooks on atomic physics [5]. In a very simplified picture, the electrons surrounding the nucleus and balancing its charge to yield the neutral atom are arranged in "electronic shells", the stronger the binding energy the smaller the radius of the electronic shell (or more precisely the mean radius of the electron density distribution). Following the standard nomenclature, see Fig. 1, x-rays resulting from electronic transitions to the most deeply bound electronic levels in an atom, the K shell, are called K-x-rays with indices added to label the origin of the electron filling the empty available state in the K-shell after an electron had been removed by collision or by photo effect. The most prominent transitions are the two K_α-lines which combine the two allowed L-levels with the K-level. With typical x-ray detection setups, commercially available, the two K_α-lines are resolved in their energy only for elements higher in Z than the rare earth elements. The K_β lines, transitions between the less

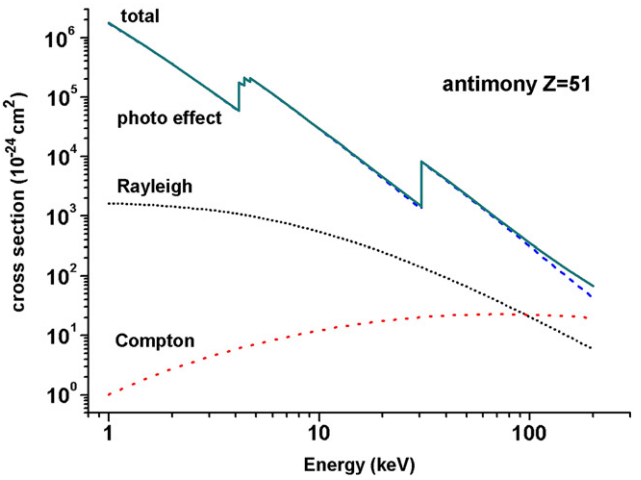

Fig. 2. Cross section for the interaction of photons in antimony. The Rayleigh, Compton and absorption cross sections are given. The linear mass absorption coefficient is easily calculated from the total cross section knowing the composition and density of the material.

bound M or higher order levels and the K-level, have higher energies and are associated with roughly a factor of 5 less intensity than the K_α-lines. The x-rays to the less bound levels, are considerably less energetic, such as the L-lines or higher order lines, and more complex in their splitting into a variety of sub-lines as can be figured out from Fig. 1.

The effectiveness in the detection of emitted characteristic x-rays for elemental identification is restricted by at least two factors, first from simple atomic physics, by which the alternative way of de-excitation, the emission of Auger electrons dominates for low transition energies, and second by loss through absorption in material in the path between the object (source of emission) and the detector. The fraction of x-rays being emitted, the so-called fluorescence yield, is very low for light elements and increases with increasing Z beyond a 90% level at around $Z = 55$ according to the empirical calculation by Bambynek et al. [6]. It illustrates why it is so difficult to accurately determine low Z elements.

A typical cross section, i.e. the probability for the absorption of photons in the energy range of interest in this context is given in Fig. 2, the data for the figure are taken from the data base as provided by NIST, Ref. [7]. It shows the cross section for elastic or Rayleigh scattering, the inelastic or Compton scattering, the cross section for photo electric effect, and the total cross section. As is seen, the absorption according to the photo effect is the main part and yields the information on the absorbing elements reflecting again the electronic structure of the atom (see Fig. 1) with the sharp increases ("edges") in the cross section when the photon energy exceeds the binding energy of the next more deeply bound electronic level.

The cross section for absorption as illustrated in Fig. 2, which is easily transformed into the mass absorption coefficient, usually given in cm^2/g, presents the basis not only for determining the elemental composition of an object by x-ray fluorescence but it also is the basis for the contrast in imaging techniques. Its changes with the elements are used in element-sensitive imaging by absorption or scattering techniques. The basic contrast results from variations in the electron density of the material under study. Both the coherent (based on Rayleigh scattering) and incoherent scattering (based on the Compton effect) increase with Z, the coherent part roughly with Z squared, and the incoherent part roughly linearly with Z: A strong elemental enhancement is therefore achieved when the absorption through the photo electric effect can be employed, which increases with roughly Z^4 to Z^5. For details on the various partial cross sections, see various text books [8].

2.1.2. Production of x-rays by x-rays

In the case of excitation by monochromatic x-rays, the intensity of the fluorescence line or the contrast in absorption drastically changes from below to above an absorption edge of a specific element. At synchrotron radiation facilities, beam lines equipped with monochromator crystals provide well-focused and collimated x-ray beams to excite x-ray fluorescence with high elemental sensitivity by changing the energy of the exciting radiation from above to below the respective absorption edge. Since the monochromatization is based on coherent scattering in reflection on crystal

planes ("Bragg reflection" conditions), higher-order reflections may be a source of error in the case of trace elements if the higher-order x-rays are not totally suppressed.

In the case of x-ray tubes such elemental sensitivity is very much restricted to filtering means. With tubes, monochromatic x-rays, superimposed on the continuous Bremsstrahlung spectrum, are only produced by excitation of the characteristic x-rays with suppression of perturbing x-ray lines such as the K_β lines (see above) by "critical" absorption. A critical absorber in this case is a filter with its absorption edge at an energy between the K_α and the K_β lines of the anode, e.g. a nickel (Ni) filter for a copper (Cu) anode tube. Above $Z = 23$, i.e. vanadium (V), any combination of an anode of element Z with a filter of element $(Z - 1)$ may improve the performance of a filtered source. At higher Z, a filter with $(Z - 2)$ might be a better way to filter out unwanted parts of the source spectrum.

According to Fig. 2, a sizeable fraction of the incoming radiation, whether mono-energetic or continuous in energy, is deposited within the material, within the object, without the production of the characteristic x-rays (i.e. "fluorescence radiation"). This part consists of the energy delivered to the photo electron released in the absorption process in excess to its binding energy and the fraction lost in photo effect processes on less-bound electrons (cf. the extrapolation of the absorption underneath the step-like increase at the edge) as well as on the fraction resulting from the Auger electron emission as the alternative process to fluorescence. Additionally, the processes following the fluorescence (XRF) or Auger-electron emission are further sources of unwanted energy deposition. All these unwanted parts of transferred energy are useless in this context because they do not contribute to any exploitable signal. On the other hand, they may give rise to material modifications (e.g. by chemical bond-breaking) which one has to minimize and keep below a tolerable limit.

2.1.3. Production of x-rays by particles

a) Cross section

The production of x-rays by particles results from the Coulomb interaction, by which an electron is kicked out from the atom due to a fast moving charged particle. The atom is ionized, a "hole" in the electronic shell is generated which is filled by a less strongly bound electron with the emission of the characteristic x-rays (or the alternative emission of an Auger electron, see Section 2.1.1). This process is well known by the name PIXE, proton (or particle) induced x-ray emission. The cross section for the "kicking-out" of the electron is typically calculated using the first-order Born approximation of scattering theory with various degrees of sophistication (Coulomb perturbed stationary states including relativistic effects, energy loss effects, and others, e.g. [9]). Nevertheless, deviations from experimentally determined cross sections may be around 10% or sometimes even larger, especially for higher Z elements and higher projectile charges because of shielding effects. The general feature is that there is a maximum cross section at around the projectile energy corresponding to the Bohr's velocity matching criterion, i.e. projectile and electron velocity in the respective atomic shell should be equal. For a given electron binding energy E_K the particle energy for the velocity matching condition is simply obtained by multiplying the binding energy with the mass ratio of the mass of the ionizing projectile m_p and the electron mass m_e, which is close to a factor of 2000 in the case of protons. Since the binding energy of the electrons increases with Z^2, and the radius of the respective electron cloud decreases with Z, a strong decrease in Z is expected for the cross section maximum of the inner-shell ionization according to a rather simplified geometrical picture. As a guideline Table 1 gives estimated cross sections at the particle's energy under the velocity matching condition for increasing Z. Additionally, the cross sections for PIXE in the "standard" mode of a proton beam of 3-MeV energy are also given, which is the mostly used beam at small accelerators for this kind of studies. These ionization cross sections by protons are compared to the photon absorption cross section by photo effect [7]. The comparison presented in Table 1 illustrates that the production cross section via photons as compared to particles (protons under optimized conditions) is higher by a factor of roughly 5 for low Z and by a factor of 100 for very high Z. It also holds in the case of less bound electrons like the L-x-ray production. That the differences are not much larger, results from the common electromagnetic interaction responsible for the processes.

With an increase of the charge of the incoming particle with elemental number Z_p, the ionization, and consequently, the x-ray production via charged particles can be increased. To first order, it should increase with Z_p^2, with shielding effects leading to a slower increase. Excitation with alpha particles at the same velocity should result in a four time higher yield as compared to protons.

Fig. 3 presents a graphical illustration of this comparison. Instead of giving cross sections at the optimized energy for each individual element Z as in Table 1, fixed energies (3 and 68 MeV, resp.) for the incoming particles are assumed. In the case of x-rays a monochromatic radiation is assumed, therefore the graphs end at that Z value, at

Table 1
Comparison of the x-ray production by protons (PIXE) and by photons.

Element symbol	Z	Electron binding energy E_K (keV)	Proton energy (for matching) MeV	σ_{PIXE} (10^{-24} cm^2)	$\sigma_{PIXE(3\ MeV)}$ (10^{-24} cm^2)	$\sigma_{photo\ effect}$ (10^{-24} cm^2)
Al	13	1.56	2.8	30000	30000	177000
Fe	26	7.1	13	1500	400	37000
Te	52	31.8	58	50	0.8	7600
Pb	82	88.0	162	18	0.01	2500

For some representative elements the element symbol, the element number Z, the electron binding energy in the K-shell E_K, the proton energy for velocity matching, the cross section at this matching energy, and for comparison the cross section at a proton-energy of 3 MeV $\sigma_{PIXE(3\ MeV)}$ as well as the cross section for photo effect $\sigma_{photo\ effect}$ are given for increasing Z. The ionization cross sections are adopted values from the tables in [10]. The data for photo effect are the cross section for photo absorption at a photon energy just above the K-shell binding energy of the respective element (from [7]).

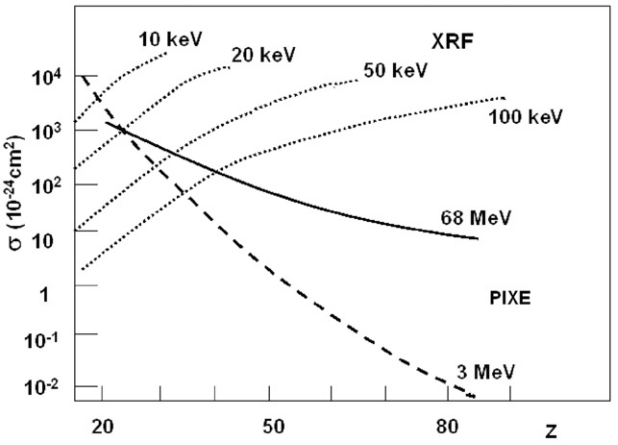

Fig. 3. Comparison of the cross section for photo absorption just above the K-edge and for the K-shell ionization by protons at 3 and 68 MeV as a function of Z. To obtain the net x-ray intensities, the cross section has to be multiplied by the fluorescence yield. In the case of photo absorption, only roughly 80% leads to K-shell ionization, the other part leads to photo effect at less bound electrons.

which the binding energy is larger than the energy of the incoming photon. The curves presented are based on the data of Ref. [7] (for x-rays), Ref. [10] (for 3 MeV protons), and Ref. [11] (for 68 MeV protons). Thus Fig. 3 illustrates how the excitation of x-rays by monochromatic x-rays and by low- and high-energy protons complement each other for a versatile usage of the produced radiation.

Applications to analytical studies, typical for the 3 different means of production are given in Figs. 4, 5, and 6. In Fig. 4, a low-energy x-ray spectrum is shown for a low-energy PIXE analysis of a glass piece from a stained glass window from the Notre Dame cathedral in Evreux. The high yield in low-energy PIXE for low-Z elements is accompanied by the low separation in energy of the various K-lines, and additionally they are intermixed with L- and M-lines originating from high-Z elements. Therefore a precise compositional analysis may be difficult due to various redundancies. However, they may be disentangled when combined with additional information such as from simultaneous RBS and PIGE (see below). Figs. 5 and 6 illustrate the much better resolved detection of high-energetic K-x-rays of medium- and high-Z elements in the presence of low-Z elements both by high-energy PIXE (Fig. 5) [12] and x-ray fluorescence (Fig. 6) [13]. The high-energy PIXE example illustrates the detection of a lead-containing (Pb) compound as powder within in a sealed glass flacon from Egypt. Such Pb-compounds were used for cosmetics (further details are given in Ref. [12]). The XRF example gives a detail in the investigation to reveal a hidden painting under the presently visible van Gogh painting *patch of grass.* The painting underneath was revealed by mapping of x-ray absorption on antimony (Sb) as identified by XRF shown in Fig. 6 [13].

Besides the wanted x-rays, certain unwanted contributions are produced, too. These are well-defined characteristic γ-rays produced in nuclear reactions (see Section 2.3 for nuclear cross sections), and continuous background radiation from various origins. The dominant contributions are bremsstrahlung from stopping of secondary electrons to which

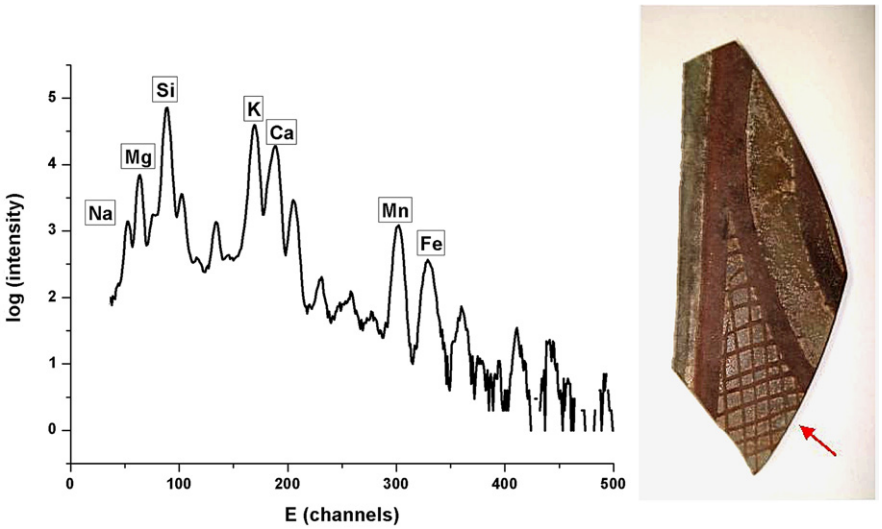

Fig. 4. X-ray spectrum measured in 3-MeV proton excitation (low-energy PIXE) of a piece of a stained glass window shown to the right. The arrow marks the position where the proton beam was directed onto the central region of a glass edge. We thank C. Loisel from the Laboratoire de Recherche des Monuments Historiques LRMH, Champs-sur-Marne for supplying the piece of glass.

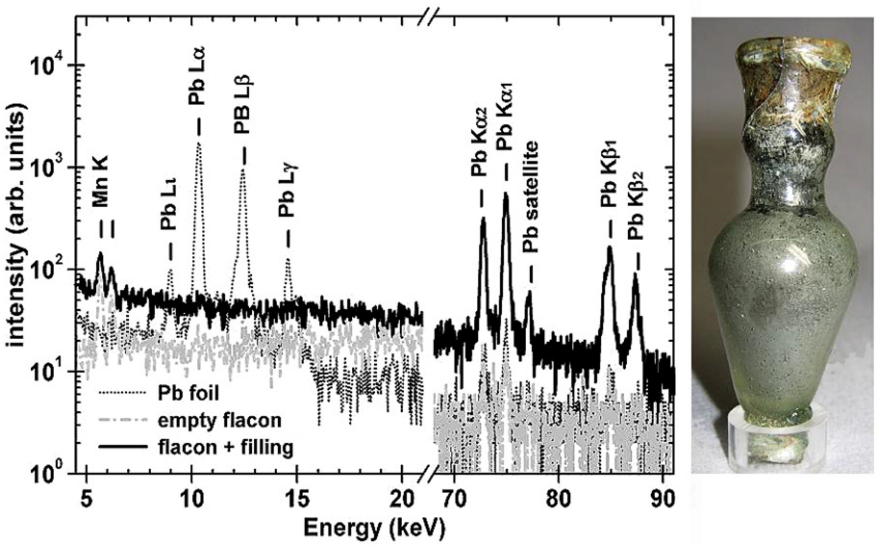

Fig. 5. High-energy PIXE on a sealed glass flacon from Egypt, partly filled with a powder of a lead (Pb) compound, and a Pb foil for comparison [11]. We thank A. Grimm from Staatliches Museum Ägyptischer Kunst München for letting us use his photograph of the flacon, shown at the right, for this review.

the maximum possible energy T_m has been transferred from the projectile (from simple elastic collision mechanics, this maximum energy is given by $T_m = 4(m_e/m_p)E_p$), atomic bremsstrahlung emitted from the stopping of the incident particle, and finally Compton scattered γ-rays resulting from nuclear reactions. The atomic bremsstrahlung corresponds to the major radiation output of continuous energy in x-ray tubes. In the case of PIXE it is largely suppressed, since the production is governed by the inverse mass to the 4th power. This mass dependence may be an additional argument for using ^{4}He (alpha)-particles instead of protons for PIXE when being available and when applicable (see further down).

b) Stopping of exciting particle

Besides the production of the useful x-rays, a big concern is the useless extra energy being deposited in the material or object. *Does it leave behind a visible change or a non-tolerable hidden change*? In the typical form of PIXE being

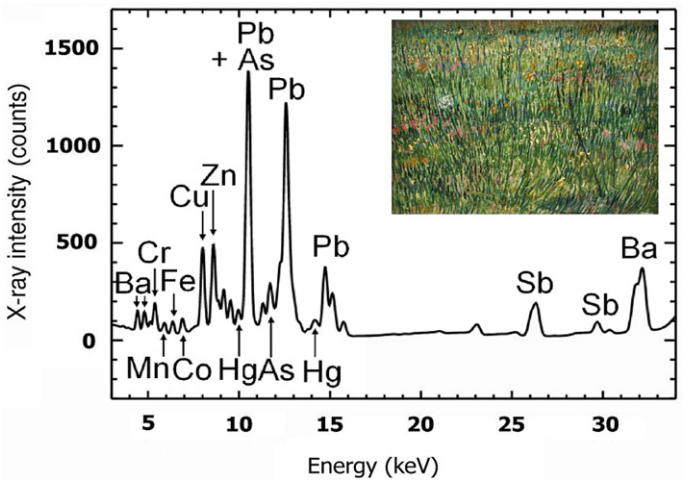

Fig. 6. Monochromatic synchrotron radiation XRF for the detection of medium to high Z elements. The x-ray spectrum reveals the occurrence of antimony (Sb) which results from the hidden painting underneath the present version. By mapping of the x-ray absorption on Sb in the XANES region, details of the hidden painting became better "visible" than in earlier radiography (for details see Ref. [13]). We thank the authors of Ref. [13] for letting use their data for this review.

routinely used (at around 3 MeV), the energy brought into the material by the particle is nearly totally released within the layer corresponding to the particle range. The energy is mainly transferred to electrons (by ejecting and exciting electrons), called electronic stopping, and only near the end of the slowing down process transferred to constituent atoms as a whole, called nuclear stopping. The electronic stopping leads to the wanted x-ray emission, but to secondary electrons as well resulting in additional photons and phonons. The nuclear stopping leads to displacements of atoms and lattice defects.

In principle, the stopping of charged particles in matter is widely understood. At low velocities, the incoming ion gets neutralized, so that the interaction occurs between neutral atoms, resulting in ballistic collisions (nuclear stopping), which decreases inversely with the energy E_p of the incoming particle as $1/E_\mathrm{p}$. With increasing ion velocity v_p, the electronic stopping takes over which is well described by the Bethe–Bloch formula. It describes the energy loss per unit length by electronic stopping in a material as being proportional to the number of electrons provided by the constituent atoms, i.e. by Z, and the atomic density in the material N (in atoms/cm^3), by the square of the charge of the incoming ion, i.e. Z_p^2, and the square of the inverse of the velocity of the incoming particle. The derivation of the Bethe–Bloch formula, given here in a simplified version, can be found as treated by Lehmann [14],

$$-\mathrm{d}E/\mathrm{d}x = 4\pi Z_\mathrm{p}^2 e^4/v_\mathrm{p}^2 \cdot N \cdot Z \cdot \ln\bigl(2m_\mathrm{e}v_\mathrm{p}^2/I\bigr) \tag{1}$$

(I is an average ionization energy $I = 11.5Z$ eV).

From this energy-loss formula one obtains the total range by integration over the path until the ion energy is used up, i.e. the ion comes to rest.

In the case of PIXE with protons in the energy range of 1 to 4 MeV, as the typical energy of the incident particle used at small accelerators for ion beam analysis purposes, the proton range is slightly larger than the sensitive thickness for the x-ray production and detection, and is in the order of 100 μm and less. Such a range matches the thickness of paintings, glazes and relevant layers associated with ceramics, glasses and similar objects of our cultural heritage, but it can be too short to be used in cases of covering layers either as protective coating or as patina from aging due to chemical reactions on the surface.

c) Materials modifications

When the energy loss per unit length is plotted over the incoming energy, as is illustrated in Fig. 7 for protons in Cu, according to [15], one realizes that the maximum energy deposited within the material under investigation falls directly into the sensitive depth region for the x-ray excitation in the highly used energy regime of the incoming proton of around 3 MeV. The highest concern for this energy input must be given to organic material, less to insulators, ionic crystals, oxides, etc., materials like in precious stones, minerals, etc. Metals are considered to be the least effected class of materials. In metals, electronic excitations rapidly relax, but atomic disorder due to atomic displacements

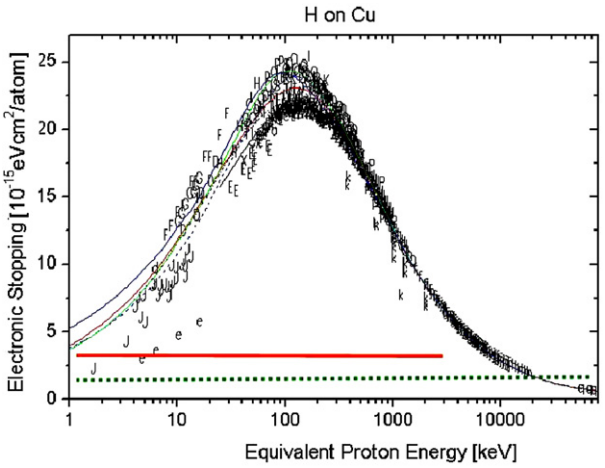

Fig. 7. Energy transfer ("stopping power"), $\mathrm{d}E/\mathrm{d}x$, for protons in copper. The graph contains a large collection of experimental data as put together by H. Paul which may be found on http://www.exphys.uni-linz.ac.at/stopping/. The solid bar (in red) indicates the relevant region of the energy deposition for 3-MeV protons in conventional low-energy PIXE, while the dotted line (in green at the bottom) indicates the total region for 68-MeV protons, the energy when entering the object is at the right end of the respective lines (conversion: for copper 10×10^{-15} eV cm^2/atom corresponds to 84.6 keV/μm). (For interpretation of the references to color in this figure legend, the reader is referred to the web version of this article.)

may take some time to anneal at ambient temperatures, mainly via diffusion processes. Since paintings often consist of organic components, binder, protective layers, organic pigments, and others, they deserve and have received the highest attention in terms of visible side effects of analytical techniques with ions such as PIXE with 3 to 4 MeV protons. Various groups have investigated the damage effects using mock-up layers. Neelmeijer et al. [16] state a limit for a safe application to paintings of 0.5 nA/mm^2 of a proton beam at 4 MeV for 30 seconds corresponding to a power of 60 mW s/mm^2 when analyzed in open air with gas blown onto the beam spot on the painting for additional cooling. As gas, helium (He) is often used to additionally reduce absorption of the low-energy x-rays. The power is about the same power as in an illumination with a current laser pointer, commercially available, of 1 mW for 60 seconds.

Comparing the energy deposited by protons of 3 to 4 MeV with the energy deposited by x-rays of 10 keV, the unwanted energy deposition is about two orders of magnitude higher in the case of protons as compared to x-rays. For pure organic material, like for varnish layers, it even may exceed three orders of magnitude, since the mean attenuation length for photons in such low Z material is much larger than the proton range. As soon as a significant amount of inorganic pigment is mixed in, the deposited energy equals roughly the incoming energy of the respective exciting particle, proton or photon, respectively. It means that in low-energy PIXE the energy input is approximately a factor of 100 higher as compared to low-energy x-ray analysis.

As outlined at the beginning of this section (see Table 1), it is advantageous to go to higher exciting particle energies for the detection of higher Z elements because of the higher ionization cross section. Additionally, the higher energies bring along several favorable features:

(1) The energy deposition in the top part of the object is reduced and thereby any side effects are further minimized: Using protons with energies around 70 MeV reduces the deposited energy within the chosen representative 100-μm layer of organic material by a factor of 20 down to 150 keV. Like in Ref. [16] for low-energy PIXE, Denker et al. have tested the side effects for the high-energy PIXE and demonstrated the much safer use of this technique as compared to the low energy even for very radiation sensitive organic layers [17]. Such an energy is only a factor of two to five higher than a deposited x-ray energy for x-ray fluorescence at K-edges of high Z elements. Of course, at the end of the total range, the same energy per unit length is deposited as in low energy PIXE.
(2) A "look" more deeply into the object due to the longer range is possible, even through "dead" layers: The gain in depth is limited by the absorption length of the produced x-rays to be detected. Material beyond the absorption length but still within the range of the particle will be "invisible". Here the detection of higher energetic gamma-rays resulting from nuclear reactions may take over (see Section 2.3).

(3) The longer range may be useful in obtaining higher x-ray yields when the respective element is distributed over the full detectable depth: If applicable the longer range reduces the applied dose of energy deposition, thus reducing side effects further.

2.2. The atomic mass

The incoming charged particle not only interacts with the electrons of the atom but also with the nucleus with mass number A of the atoms within the object. This elastic collision, called Rutherford scattering, provides a quantitative analytical technique due to the well-known characteristics with limitations only by separating contributions from different elements in overlapping processes. The process is energetically governed by the involved masses in the kinematics. Thus the element number Z enters into the description of the kinematics only indirectly by the empirical relation between element number Z and mass number A for stable isotopes ("valley of stability"). A simple relation between Z and A for the stable nuclei is derived from the Bethe–Weizsäcker mass formula (see textbooks on nuclear physics, e.g. [8]). The element number Z is about half the mass number A for light elements and becomes increasingly less than that for higher masses. This is expressed more quantitatively according to Eq. (2). The most stable nuclei for a given mass A are the ones with the integer Z being closest to the minimum Z_0 derived from the mass formula for A as a function of Z:

$$Z_0 = A/\left(1.98 + 0.015A^{2/3}\right) \tag{2}$$

Due to the well-known interaction, the cross section can be calculated and a quantitative analysis is easily performed in principle, provided the necessary conditions are fulfilled. Here, a direct dependence on Z enters as Z^2 in the absolute cross section, i.e. in the intensities as a result of the Coulomb interaction.

Two closely related analytical techniques are based on this Rutherford scattering process: Rutherford backscattering spectroscopy, RBS, or the complementary variant called Elastic Recoil Detection Analysis, ERDA. Because of the kinematics, RBS is best applied for the detection of heavy elements in matrices of light masses, while the forward recoil in ERDA, out of the sample ("kick-out"), is easier realized for light elements. In the latter case the detection of the recoiling atom is almost impossible in open air. Only in very special and highly sophisticated experimental setups, the detection of e.g. hydrogen has been realized [18]. In the former case of RBS, the setup at AGLAE (Accelerateur Grand Louvre Analyse elementaire) at the C2RMF routinely operates with objects in open air. This was made possible by thin vacuum-tight window foils made out of Si_3N_4, and with very compact geometry with additionally flooding of the volume of open space, the particle has to traverse to and from the sample, with helium gas for reduced absorption. A detailed description has been given in earlier publications [18,19]. A comment should be added here to give the reason why heavy ions are not well suited for analytical purposes because of the enhanced energy loss in open air and the enhanced energy deposition in the vacuum-tight window foil so that it can not withstand a high enough particle flux needed for the experiments (see Eq. (1)).

The information on the mass, and by that, on the element as a constituent or as a trace element, is obtained by measuring the energy of the backscattered particle, e.g. the proton. The highest energy is found for backscattering on heavy elements on the surface, while collisions with lower mass elements lead to higher energy transfer, and backscattering particles on atoms deeper within the sample have experienced an energy loss on the way in, as well as on the way out, of the sample. Thus unfolding the measured energy spectrum yields information on the depth distribution of the elements, provided one can solve the various redundancies. It is easily realized that this technique is well suited for investigating layered structures near the surface of dimensions up to several ten μm.

The necessary condition under which a quantitative analysis is feasible is that the incoming energy stays below the Coulomb barrier, the potential "hill" which results from the repulsive Coulomb potential the incoming proton "sees" when approaching the nucleus and the attractive nuclear potential when the proton actually reaches the nucleus. For protons and alpha-particles the Coulomb barrier is plotted in Fig. 8. However, due to sub-Coulomb barrier nuclear reactions, the Coulomb barrier is only a guideline for the applicability. As a rough estimate a second line, 2 MeV lower in energy, is also given in the figure for the proton energy, below that energy limit the possible deviations are very small. Higher energies lead to nuclear reactions which may also be used favorable in some cases (see Section 2.3). In cases, where the energy dependences of the total cross sections are known, they may be used for a depth distribution analysis as well (for details see [20]).

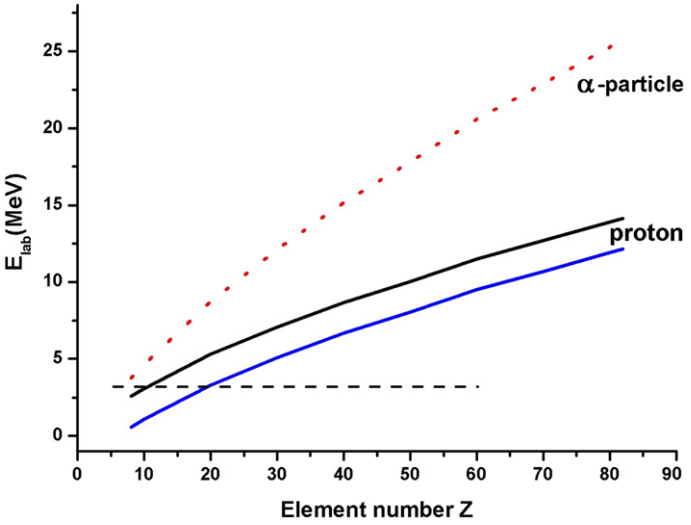

Fig. 8. Coulomb-barrier for protons and alpha-particles as a function of Z. The incoming particle energy is plotted in the laboratory frame. For protons, a limiting line for sub-Coulomb nuclear reaction processes is given, too. According to [20], deviations from Rutherford-like behavior should be on the % level with an energy below such a limit. The horizontal dashed line marks the typical energy for low-energy particle beams used in cultural heritage studies.

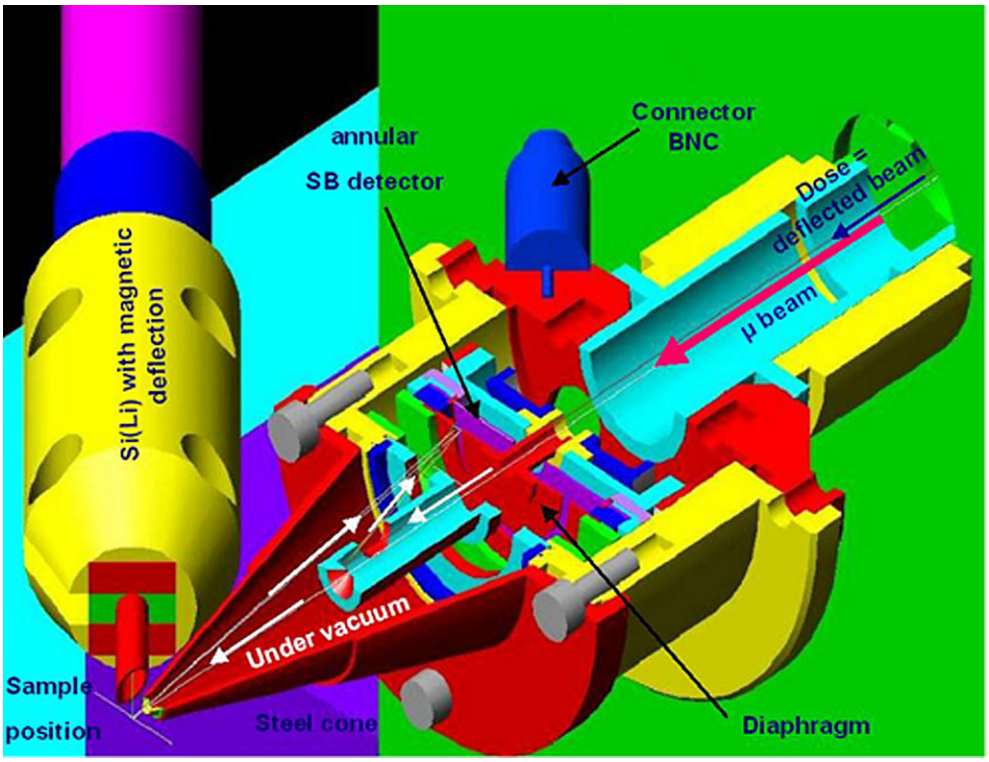

Fig. 9. Experimental setup AGLAE for PIXE and RBS with the objects at "open air". An additional Si(Li)-detector is used for high-energy x-rays and a Ge-detector for γ-rays.

Various low-energy PIXE facilities have set up microbeam focusing down to a few 10s of micrometers. Taking the depth resolution in RBS, which may be in the order of 20 nm depending on the energy resolution of the particle detectors, the thickness and homogeneity of the vacuum exit windows, the travel distance through air, the combination

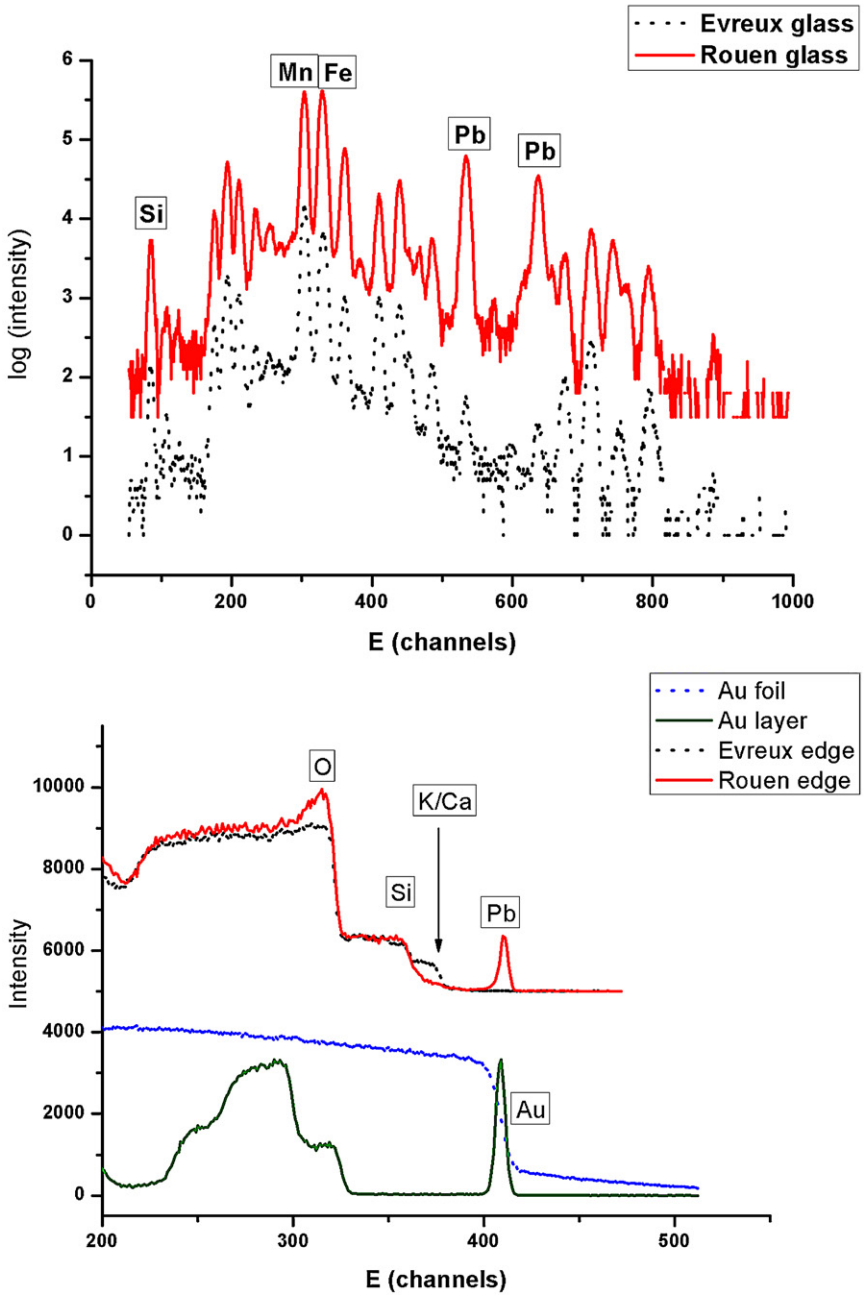

Fig. 10. PIXE (top) and RBS (bottom) with protons on pieces of stained glass windows from the cathedral Notre Dame in Evreux and from the church St. Ouen in Rouen. The Rouen glass piece shows a high Pb contribution in the x-ray spectrum. Compared to Fig. 4, the spectra shown here were taken with the high-energy detector. The RBS spectrum reveals that the Pb contribution results from the surface only (less than 400 nm). To illustrate that only a thin layer contains Pb, RBS spectra for gold (Au) on a thick foil and on a thin Au layer on mylar are presented for comparison as well.

of RBS together with the x-ray detection of PIXE has proven to be a very versatile and powerful analyzing technique. As an example, we show the setup at AGLAE at the C2RMF at the Louvre in Fig. 9 as it is routinely used for analyzing art objects [19]. In Fig. 10 a compositional study of glass pieces from stained glass windows from the cathedral in Evreux and from a church in Rouen is presented illustrating the complementary information obtained with PIXE and RBS [21]. In the PIXE spectra (a), the complexity in the x-ray spectra is obvious with the many neighboring and

overlapping low-energy K-, L- and M-lines of the elements from sodium (Na), magnesium (Mg), aluminum (Al), silicon (Si), phosphorus (P), potassium (K), calcium (Ca), titanium (Ti), manganese (Mn), iron (Fe), rubidium (Rb), strontium (Sr), and lead (Pb), the list not being complete. Only with the help of the RBS spectrum (b) did it become clear that Pb is not a constitutional part of the bulk glass but rather a contaminant on the surface, with a layer of less than 400 nm. It could be due to a treatment of the surface carried out by the artist or a conservator later on or be the result of surface reactions under weathering conditions where the lead framing could be the source of the lead.

In cases where alpha-particles are available with appropriate energies, the shorter range and the higher yield for inner-shell ionization may be favorable in a combined PIXE and RBS analysis. In x-ray production one is less perturbed by background from bremsstrahlung and usable intensities are obtained for higher-Z elements for the K-shell excitation; in the RBS, the alpha-particles yield a higher resolution for surface layers, naturally at the expense of less deep range [22].

2.3. Different isotopes of the same element

The big advantage of PIXE is the high cross section of the inner-shell ionization for light elements, necessary for the x-ray production, see Fig. 3. However, it goes along with low transition energies for the emitted x-rays for these low Z elements and a large non-radiative de-excitation ("Auger electron emission"). For example, the fluorescence yield for the Na K-line is only on the 1% intensity level [6]. A feasible alternative is to detect gamma rays produced in nuclear reactions, the derived method being called PIGE. In such a case, the element is identified by a specific isotope of the element Z with a specific mass number A. Accordingly, for low Z element, setups for low energy PIXE combined with RBS are additionally often equipped with a high energy gamma-ray detector. A typical example is the quantitative analysis of Na performed by analyzing the intensity of the 439-keV γ-line from the ^{23}Na $(p, p'\gamma)$ reaction (sub-Coulomb barrier nuclear reactions), often used in the analysis of glasses [23]. There are a few resonance-like nuclear reactions which may even be used for concentration profiling (for details see [20]).

For low-energy PIXE, nuclear reactions are no longer accessible at Z larger than around $Z = 20$, as can be seen from the Coulomb barrier plot in Fig. 8.

The often much higher energies of γ-rays resulting from nuclear reactions make them attractive for analyzing small amounts of trace elements, especially when they can be excited in larger sample depth than the absorption length of the normally used x-rays. For high-energy PIXE a possible type of reaction to be used for identification is the fusion-evaporation reaction where the high-energy proton is "absorbed" by the hit nucleus and the excited nucleus gets rid of the excitation energy by evaporating a few nucleons, mainly neutrons, since the evaporation of charged particles is suppressed by the Coulomb potential ("barrier"). The cross sections for this (p, xn) $(x = 1, 2, 3, \ldots)$ reactions are in the order of the geometrical cross sections, i.e. $\sigma = \pi R^2$ with the nuclear radius $R = r_0 A^{1/3}$ ($r_0 = 1.27$ fm) (see [8]). From the mechanism, the yield shows maxima, roughly 15 MeV apart, the first one at around 10 MeV, still suppressed by the Coulomb barrier for the incoming proton. The second one at around 25 MeV is typically the highest. Beyond the $3n$-maximum at around 40 MeV, the cross sections become highly reduced again due to competing reactions and mechanisms (see Fig. 11 sketched according to the example taken from Ref. [24]).

Such (p, xn)-reactions can be used in two different experimental arrangements: (i) by detecting produced γ-rays in-situ in parallel to the detection of the x-rays with a separate γ-detector (PIGE) and/or (ii) by activation analysis following the irradiation. An example for the first is given in Ref. [17].

While activation analysis may be used as a means to detect specific isotopes and thereby elements, one has to be aware of the radioactivity being produced. The same holds as a side effect in the detection of x-rays since nuclear reactions occur simultaneously. However, due to the high sensitivity and selectivity in counting high-energy x-rays and γ-rays the total number of produced radioactive nuclei is small and negligible after a few half lives of the radioactive decay. The example used in Ref. [14] may illustrate that. A copper containing silver coin, 0.5 mm thick, was analyzed with a 68-MeV proton beam of 0.1 picoampere for 200 seconds. It yielded roughly 600 atoms per second, or a total of 120 000 ^{61}Cu atoms after 200 s, which decay into the stable nickel isotope ^{61}Ni with a half life of 3.5 h, which corresponds to an activity of 30 Bq. After a few hours the activity fell below the background level and could no longer be detected.

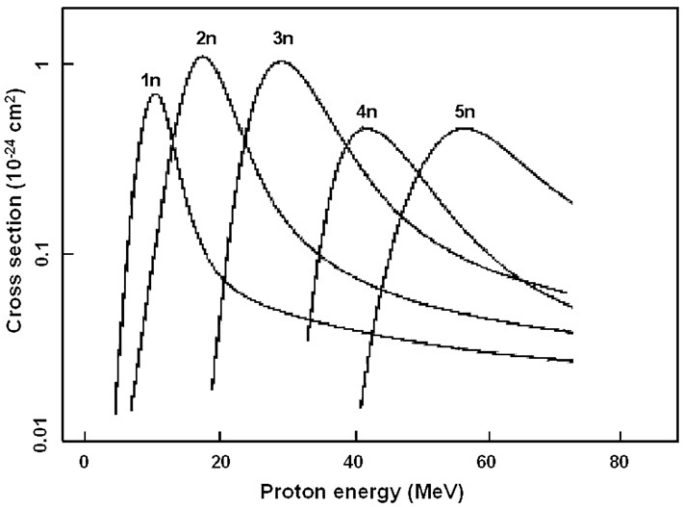

Fig. 11. Typical behavior of the cross section for fusion-evaporation type (p, xn) reactions $(x = 1, 2, 3, 4, 5)$ for use for PIGE at high proton energies. The graphs are redrawn from data presented in Ref. [24] for tellurium isotopes.

3. Accelerators for the production of x-rays as a radiating source

In the XRF technique, characteristic x-rays are produced up to a limit given by the specific absorption edge; any element with an edge lower in energy will be excited. In PIXE, all elemental characteristic x-rays are produced simultaneously yielding a good mapping of all the elements. This is favorable, of course, only for K x-rays where the x-ray lines are well separated and interference with lines from unknown elemental sources can easily be solved. For low-Z elements and for L x-rays this often leads to overlapping lines, which may be difficult to untangle in quantitative analysis. This different feature for XRF and for PIXE illustrates a very useful complementary approach: an elemental overview with PIXE and a decisive determination with a monochromatic x-ray source. Such decisive measurements are possible at present at large size synchrotron facilities only. However, they often additionally offer the possibility to determine the chemical form as well with techniques such as the two variants of x-ray absorption spectroscopy: (i) X-Ray Absorption Near Edge Spectroscopy (XANES); and (ii) Extended X-Ray Absorption Fine Structure (EXAFS). The study of the hidden painting within the van Gogh painting by Sb EXAFS in addition to the XRF shown in Fig. 6 is a recent example [13]. In a few years from now, monochromatic high-energy x-rays may become available in small laboratories as well (see below).

Meanwhile, PIXE facilities may be used as a source of "mono-energetic" x-rays by exciting characteristic x-rays and employing critical absorption for "cleaning" the x-ray source. Such a source emits into 4π which may additionally be very useful for imaging purposes.

A rough estimate of the yield of such a usable photon source shows, it delivers more than 10^{12} photons/s emitted into a solid angle of 4π originating from a source of 0.01 cm^2 or less depending on the primary microbeam quality. Using arsenic as a target with a proton beam of 100 nA at 24 MeV (velocity matching energy, see Table 1), such a photon source may be realized with germanium (Ge) as critical absorber. With a K-shell ionization cross section of 500×10^{-24} cm^2 background radiation originating from nuclear reactions and follow-up processes are, at least, a factor of 500 less in intensity because of the nuclear cross sections. However, in cases of quantitative trace element analysis these other sources have to be considered and may limit the sensitivity. This scheme would be applicable for other x-ray energies as well. The example arsenic was chosen since, at 3 MeV, it has been employed successfully already at AGLAE [19], but because of the lower cross section, a much higher proton beam current had to be used. The technique was applied to lower the sensitivity limit for the analysis of platinum as trace element within gold by strongly reducing the excitation of the Au L-lines [25].

According to Fig. 3 and the discussion presented, it would be advantageous to have all three accelerator-based x-ray production means available for analyzing cultural heritage objects, low-energy PIXE for low-Z elements, high-energy PIXE for an improved K-x-ray production including some PIGE specialties for information from even deeper

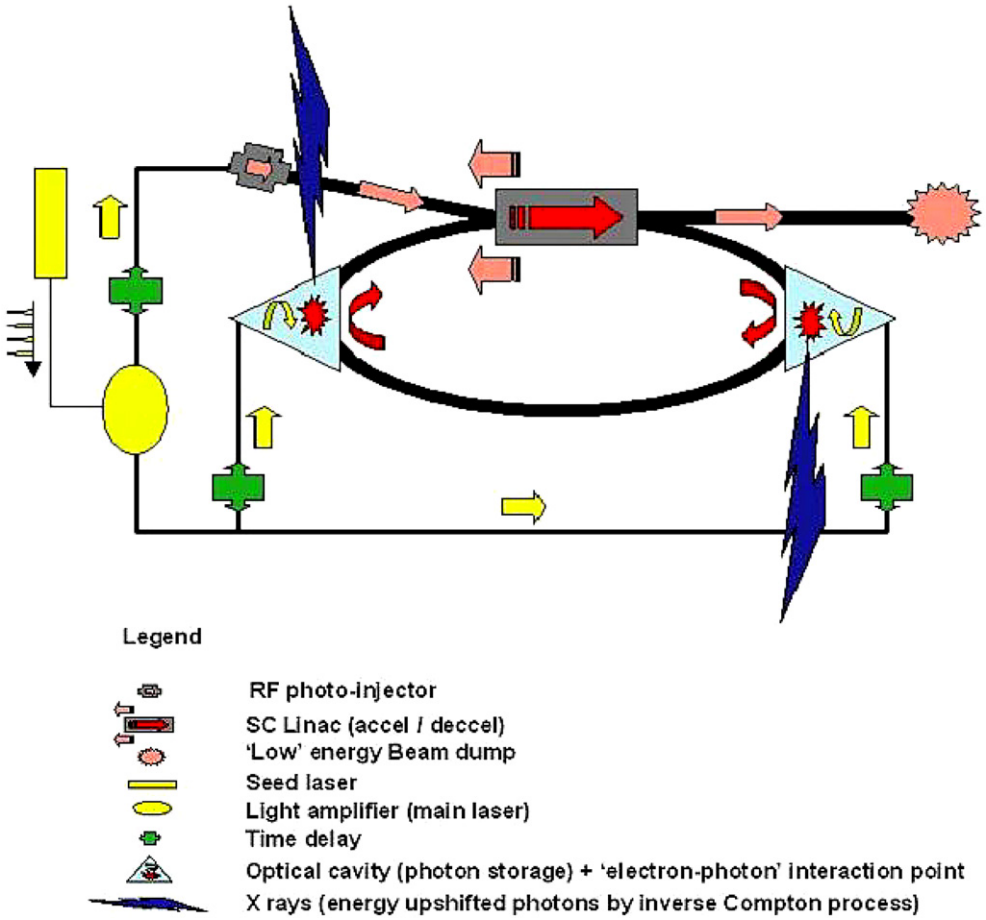

Fig. 12. Sketch for a possible high-intensity, monochromatic high-energy x-ray source ("Inverse Compton Source") with an energy recovery LINAC for the electron beam and two laser cavities.

inside the object, and for XRF high-energy monochromatic and tuneable x-rays. The XRF with high-energy x-rays is available at beam lines at the large-scale synchrotron facilities. Like the low-energy PIXE, a small size x-ray source achievable for museum laboratories may soon be realized as an Inverse Compton Source for quasi mono-energetic, tuneable x-rays, as being presently developed for various applications.

In a short and simple description, the concept of such an x-ray source is based on a head-on collision of a well-defined electron beam of several ten MeV and a well-defined photon laser beam of μm wavelength or shorter (well-defined means in the full 6-dimensional phase space, i.e. transverse space and momentum as well as the longitudinal coordinates, time and energy). This way the wavelength of the incoming photon is shortened by the relativistic energy factor squared of the primary electron γ^2 and the energy is increased accordingly as approximately given by

$$E_x \approx 2\gamma^2 E_{\text{photon}}(1-\cos\Theta_{\text{photon}})/\left(1+\gamma^2\Theta_x^2\right) \tag{3}$$

(Θ_{photon} is the angle between electron and laser beam, Θ_x is the angle between electron beam and emitted x-ray, γ is the ratio of the total energy to the rest mass energy).

As the result such a source delivers very mono-energetic tuneable x-ray photons of keV range emitted into a small cone with an opening angle given by the relativistic energy factor $1/\gamma$ and with a high degree of coherence, most useful for imaging and tomographic applications.

With such a system, a selectiveness will be reached by adjusting the energy according to the wanted absorption edges. It would help to cover the full range in Z and thereby in energy for those analytical purposes, for which high sensitivities or low detection limits are needed and asked which is not only limited to studies on objects of our cultural heritage, but in many other fields relevant for our society as well. A possible realization is sketched in

Fig. 12 according to design studies presented and discussed at the International workshop on Inverse Compton Sources 2008 [26]. A more detailed study on a practical system in relation to cultural heritage applications is part of this special issue [27].

On a longer time scale, there may even be a small laboratory-sized high-energy PIXE version possible based on the production of high-energy protons by femtosecond high-power lasers. While the production of such high-energy particles, electrons, protons and higher mass ions have been demonstrated [28] it will take some time to develop this scheme into a usable system for stable operation and with the size of a microbeam.

4. Summary

We have tried to illustrate that accelerators can be used with great advantages for a thorough analysis of cultural objects with perspectives for facilities which will be achievable even for "small" laboratories near a museum without having difficult transports of artwork to large facilities. As is shown in Fig. 3 three ways of x-ray production complement each other favorably, the low-energy PIXE using typically 3 MeV protons, the high-energy PIXE, the exact energy is not critical as long as it is well-above about 40 MeV, and mono-energetic x-ray sources with variable energies up to 100 keV. The systems discussed are not intended and will never replace easy-to-handle portable systems for field studies. Such studies with the devices brought to the object are as useful and as needed as the detailed studies performed on objects brought to the accelerators nearby or the large-scale facilities elsewhere.

Acknowledgements

H.-E.M. is very grateful to M. Menu who made his visit to the C2RMF possible, and to Ph. Walter as the scientist in charge for the planning of an intense Inverse Compton Source for the many fruitful discussions on the perspectives of such a new x-ray source for cultural heritage investigations.

References

[1] A. Gianoncelli, et al., X-Ray Spectrom. 35 (2006) 365.
[2] W. Eberhardt, B. Kanngiesser, I. Reiche (Eds.), Synchrotron Radiation in Art and Archaeology 2006, Appl. Phys. A 90 (2008).
[3] J.-C. Dran, et al., Nucl. Instrum. Methods Phys. Res. B 219–220 (2004) 7.
[4] H.G.J. Moseley, Philos. Mag. 26 (1913) 1024.
[5] B.H. Bransden, C.J. Joachain, Physics of Atoms and Molecules (Paperback), 2nd ed., Prentice Hall, 2003.
[6] W. Bambynek, et al., Rev. Mod. Phys. 44 (1972) 716.
[7] Photon cross section data from http://physics.nist.gov/cgi-bin/Xcom/xcom2.
[8] P. Marmier, E. Sheldon, Physics of Nuclei and Particles, vol. I, Academic Press, New York and London, 1969.
[9] W. Brandt, G. Lapicki, Phys. Rev. A 23 (1981) 1717.
[10] H. Paul, J. Sacher, At. Data Nucl. Data Tables 42 (1989) 105.
[11] A. Denker, et al., X-Ray Spectrom. 34 (2005) 376.
[12] A. Denker, A. Grimm, in: S. Klein, S. Laue (Eds.), Archäometrie und Denkmalpflege – Kurzberichte, 2007, pp. 18–20.
[13] J. Dik, et al., Anal. Chem. 80 (2008) 6436.
[14] Chr. Lehmann, Interaction of Radiation with Solids, Series Defects in Crystalline Solids, vol. 10, North Holland Pub. Com., Amsterdam, New York, Oxford, 1977.
[15] H. Paul, on http://www.exphys.uni-linz.ac.at/stopping/.
[16] C. Neelmeijer, et al., Nucl. Instrum. Methods Phys. Res. B 51 (1990) 140.
[17] A. Denker, et al., Nucl. Instrum. Methods Phys. Res. B 226 (2004) 163.
[18] I. Reiche, et al., Nucl. Instrum. Methods Phys. Res. B 249 (2006) 608.
[19] J. Salomon, et al., Appl. Phys. A 92 (2008) 43.
[20] J. Tesmer, M. Nastasi (Eds.), Handbook of Modern Ion Beam Materials Analysis, MRS, Pittsburgh, PA, USA, 1995.
[21] H.-E. Mahnke, et al., in: E-MRS Spring Meeting 2009, symposium R.
[22] T. Calligaro, X-Ray Spectrom. 37 (2008) 169.
[23] J. Castaing, et al., in: G. Pfennig, et al. (Eds.), G. Weber (Publ. Ed.), Karlsruher Nuklidkarte – Commemoration of the 50th Anniversary, Office for Official Publications of the European Communities, Luxembourg, 2008, ISBN 978-92-79-09115-5.
[24] A. Hohn, et al., Appl. Radiat. Isot. 55 (2001) 149.
[25] M.F. Guerra, Nucl. Instrum. Methods Phys. Res. B 226 (2004) 185.
[26] Proceedings of the International workshop on "Compton sources for X/γ-rays: Physics and applications", in: M. Carpinelli, L. Serafini (Eds.), Alghero 2008, Nucl. Instrum. Methods Phys. Res. A (2009), in press.
[27] Ph. Walter, et al., C. R. Physique 10 (7) (2009) 676–690, this issue.
[28] H. Schwoerer, et al., Nature 439 (2006) 445.